BMC Plant Biology

RESEARCH

Open Access

Lineage-specific expansion and functional diversification of mTERF proteins sculpt organellar regulation in plants

Li Yuan[1,2], Xiushun Wang[3], Huan Lin[2,4], Long-Jiang Yu[1,2] and Wei Chi[3*]

Abstract

The endosymbiotic origin of mitochondria and chloroplasts necessitated the transfer of thousands of genes to the host nucleus, yet the evolutionary paths leading to their functional specialization in organelles remain largely unexplored. Here, we investigate this fundamental question through a comprehensive analysis of the mitochondrial transcription termination factor (mTERF) family, nucleic acid-binding proteins critical for organellar gene regulation. We find that plant mTERFs underwent substantial lineage-specific expansion, diversifying into four major clades in angiosperms. Phylogenetic reconstruction reveals a complex evolutionary history: while chloroplast-targeted mTERFs and a subset of mitochondrial ones share a red algal origin, a novel clade of mitochondrial mTERFs emerged later in seed plants. This diversification underpins functional specialization in developmental transitions, such as the shift from vegetative to reproductive growth, and in environmental adaptation. Genetic analysis in *Arabidopsis* demonstrates that mTERF10, a positive regulator of salt tolerance, acts as a negative regulator of thermotolerance, illustrating how neofunctionalization facilitates adaptation to disparate stresses. Our study elucidates the evolutionary dynamics of nuclear-encoded organellar proteins and the regulatory networks they govern.

Keywords mTERFs, Organellar gene regulation, Phylogenetic reconstruction, Functional specialization, mTERF10, Thermotolerance

Introduction

The endosymbiotic origins of mitochondria and chloroplasts were pivotal in eukaryotic evolution, fundamentally reshaping the genomic and functional landscape of the cell [1–3]. Following endosymbiosis, massive gene transfer from the endosymbionts to the host nuclear genome occurred, with the vast majority of ancestral bacterial genes either lost or relocated. This process left modern organelles with only a minimal genetic repertoire, encoding rRNAs, tRNAs, and core subunits of energy transduction systems [4–6].

While many organellar genes are of prokaryotic origin, as illustrated by organellar proteases descending from bacterial precursors [7, 8], the host also evolved

*Correspondence:
Wei Chi
chiweimr@njnu.edu.cn
[1]Photosynthesis Research Center, State Key Laboratory of Forage Breeding-by-design and Utilization, Institute of Botany, Chinese Academy of Sciences, Beijing 100093, China
[2]University of Chinese Academy of Sciences, Beijing 100049, China
[3]College of Life Sciences, Nanjing Normal University, Nanjing 210023, China
[4]Key Laboratory of Plant Molecular Physiology, Institute of Botany, Chinese Academy of Sciences, Beijing 100093, China

numerous genes essential for organellar integration [9–11]. Intriguingly, product of some of these host genes also function on across different organelles [12–14]. This pattern suggests an evolutionary strategy in which gene duplication and neo-functionalization, often involving retargeting via altered transit peptides, enabled functional diversification between mitochondria and chloroplasts. However, the evolutionary trajectories and molecular mechanisms underlying such functional divergence remain poorly understood.

As semi-autonomous organelles, chloroplasts and mitochondria possess gene expression systems that rely heavily on nucleus-encoded RNA-binding proteins [15–17]. Pentatricopeptide repeat (PPR) proteins and mitochondrial transcription termination factor (mTERF) proteins are two families of nucleic acid-binding proteins closely associated with organellar functions, both of which have undergone significant lineage-specific expansion during plant evolution [18, 19]. Among these, pentatricopeptide repeat (PPR) proteins represent a striking example of lineage-specific expansion: land plant genomes encode hundreds of PPR proteins, predominantly targeted to organelles, in contrast to only a handful found in green algae such as Chlamydomonas [18, 20–25]. The evolutionary drivers behind this remarkable expansion remain unclear. Although sometimes linked to the emergence of RNA editing, the full explanatory scope of this hypothesis remains contested [26, 27]. An alternative but still underexplored view is that the expansion of RNA-binding proteins conferred regulatory plasticity, facilitating adaptation to environmental stresses via modulating organellar activity during plant territorialization [28, 29]. In contrast, although the functional importance of the mTERF protein family is increasingly recognized, its evolutionary trajectory and functional diversification in plants remain insufficiently studied.

In this study, we focus on the mitochondrial transcription termination factor (mTERF) family, a distinct class of nucleic acid-binding proteins, to explore the evolutionary dynamics of organellar gene regulation in plants. Originally identified in animals for their role in transcription termination, mTERF proteins are now known to function as multifunctional regulators of organellar gene expression, influencing processes such as transcription, mRNA stability, translation, and ribosome assembly [30–42]. Our analyses reveal that mTERF proteins have undergone pronounced expansion in land plants compared to other eukaryotes. Phylogenetic evidence indicates that all chloroplast-targeted and a subset of mitochondrial-targeted mTERFs in land plants likely derived from the archaeplastid (common) ancestor of red algae and plants, while other mitochondrial-targeted mTERFs emerged independently during seed plant evolution. Furthermore, we demonstrate that functional diversification within the mTERF family not only fine-tunes organellar responses to environmental cues but also contributes to key developmental transitions from vegetative to reproductive growth. This finding illustrates how neo-functionalization of mTERF members enables plants to deploy distinct regulatory strategies under varying environmental conditions.

Materials and methods

Collection and identification of mTERFs

Sequences from 51 representative plant species across Eudicots, Monocots, Nymphaeales, Amborellales, ferns, lycophytes, bryophytes, chlorophytes, and rhodophytes, along with 4 animal species, were downloaded to establish a local database. The plant protein sequences were obtained from the following databases: the National Center for Biotechnology Information (NCBI, https://www.ncbi.nlm.nih.gov/), Phytozome v12.1.6 (http://phytozome.jgi.doe.gov/pz/portal.html), and the Ensembl Plants database (http://plants.ensembl.org/index.html), while the animal protein sequences were acquired from the Ensembl Metazoa (https://metazoa.ensembl.org/index.html) and Ensembl vertebrates (https://www.ensembl.org/index.html) databases (Table S1). To identify mTERF genes, we performed searches against the aforementioned plant and animal proteome sequences using the Hidden Markov Model (HMM) profile of the mTERF domain (PF02536) as the query in HMMER3 software [43] with an E-value < 0.01. The initial results were manually verified using the SMART tool (http://smart.embl-heidelberg.de/) and NCBI Conserved Domain Database (https://www.ncbi.nlm.nih.gov/Structure/bwrpsb/bwrpsb.cgi) to confirm the presence of the mTERF domain.

Multiple sequence alignment, phylogenetic analysis of mTERFs and rationale for sequence selection in mTERF phylogenetic analysis

The alignments of all full- length protein sequences were generated using clustalw2 with default settings. The maximum likelihood (ML) phylogenetic tree was constructed using FastTree software (version 2.1) with the "JTT + CAT" substitution model and 1000 bootstrap replicates. The phylogenetic tree topology was visualized using the iTOL online tool (https://itol.embl.de/) and subsequently refined with Adobe Illustrator software (version 2023). In addition, a phylogenetic tree comprising 21 representative eukaryotic organisms was constructed using the TIME TREE website (http://www.timetree.org/). To systematically decipher the evolutionary history of the mTERF protein family, we constructed multiple phylogenetic trees in a stepwise manner. Given the large number of mTERF members in *Arabidopsis* and the depth of functional studies, we first generated a phylogenetic tree of the *Arabidopsis* mTERF family (Fig. 1A),

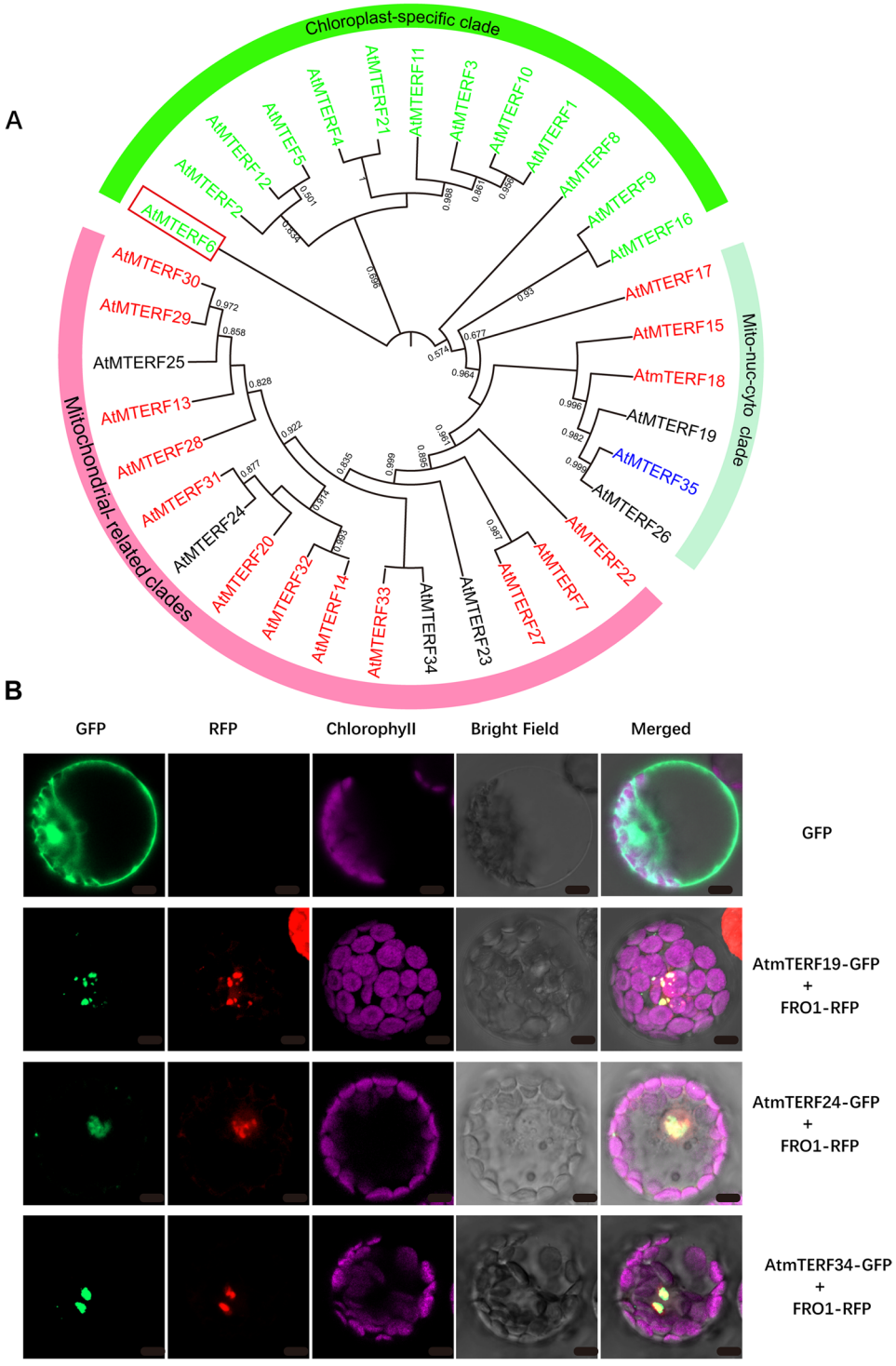

Fig. 1 mTERF proteins in *Arabidopsis thalian*. (**A**) Phylogenetic analysis of 35 mTERF proteins in Arabidopsis thaliana. Proteins are color-coded based on subcellular localization: green for chloroplasts, red for mitochondria, and blue for the nucleus and cytoplasm. Proteins with uncharacterized localization are labeled in black. mTERF6 is dually localized to chloroplasts and mitochondria. (**B**) Subcellular localization of three mTERF proteins. The empty GFP vector served as a control. FRO1-RFP, used as a mitochondrial localization control

which revealed a close association between mTERF evolution and subcellular localization. To trace the origin of different localization types, we further incorporated representative plant and animal mTERF proteins to construct a comprehensive phylogenetic tree (Figure S2). To elucidate the adaptive evolution of the mTERF family from aquatic algae to land plants, we focused on mTERF proteins from green algae, bryophytes, lycophytes, and ferns to build a phylogenetic tree (Fig. 3). Subsequently, to investigate changes in the mTERF family during the radiation of angiosperms, we constructed a phylogenetic tree using a large set of angiosperm species with green algae as the outgroup (Fig. 4), which uncovered the emergence of new subfamilies. To precisely determine the timing of origin of these new subfamilies, we performed comparative phylogenetic analyses using basal angiosperms, lycophytes, and bryophytes as outgroups, respectively (Figure S3), thereby validating their divergence nodes on a finer evolutionary scale.

Expression analysis of *mTERF* genes

Expression data pertaining to the *mTERFs* genes of *Arabidopsis thaliana*, *Zea mays*, and *Oryza sativa* were obtained from https://plantrnadb.com/zmrna/ [44]. Soybean expression data were obtained from the SoyMD database [45] (https://yanglab.hzau.edu.cn/SoyMD), while expression data for *Amborella trichopoda* and *Nymphaea colorata* were sourced from the ANAgdb database [46] (https://anagenome.cn/). The expression data for *Physcomitrium* were obtained from microarray datasets available in the ArrayExpress database (http://www.ebi.ac.uk/arrayexpress/) under accession number E-MTAB-3069 [47]. Expression data for *Selaginella* are available in the GEO database under accession number GSE123120 [48]. The expression matrix of *mTERF* genes (FPKM values) for all analyzed species was provided in Supplementary Table S4. The expression matrix (FPKM values) was log2(FPKM + 1)-transformed using TBtools, and the expression heatmaps were subsequently plotted.

Subcellular localization of AtmTERF19, AtmTERF24, and AtmTERF34

To determine the subcellular localization of selected mTERF proteins, the coding sequences of *AtmTERF19*, *AtmTERF24*, and *AtmTERF34* were amplified and cloned into the SalI site of the transient expression vector pUC18-GFP, generating C-terminal GFP fusion constructs. These constructs, together with a mitochondrial marker (FRO1-RFP), were co-transfected into *Arabidopsis* mesophyll protoplasts via PEG-mediated transformation [49]. Fluorescence signals were observed using a Zeiss LSM 980 confocal microscope.

For stable expression analysis, the PRI101:mTERF9-GFP construct was introduced into *Arabidopsis* (Col-0) via Agrobacterium-mediated transformation (GV3101) using the floral dip method [50]. Transgenic lines were selected on hygromycin and confirmed by PCR. Leaves and petioles from 5-day-old seedlings grown on MS medium were imaged using the same microscope system.

Chloroplast subfractionation and Immunoblotting

Intact chloroplasts were isolated from three-week-old seedlings (PRI101:mTERF9-GFP) homogenized in ice-cold Buffer I (0.33 M sorbitol, 0.02 M Tricine/KOH pH 8.4, 5 mM EGTA pH 8.35, 5 mM EDTA pH 8.0, 10 mM $NaHCO_3$). The homogenate was sequentially filtered through a double layer of Miracloth, a 100-μm mesh, and a 40-μm mesh. The filtrate was centrifuged at 2,000 g for 5 min at 4 °C in a swing-out rotor, and the resulting intact chloroplasts were resuspended in Buffer II (0.33 M sorbitol, 5 mM $MgCl_2$, 2.5 mM EDTA pH 8.0, 20 mM HEPES/KOH pH 7.6) [39].

To separate thylakoid membranes and stromal proteins, the chloroplasts were resuspended in Buffer III (5 mM $MgCl_2$·6 H_2O, 25 mM EDTA pH 8.0, 20 mM HEPES/KOH pH 7.6) and centrifuged at 4 °C. The supernatant was collected as the stromal fraction, and the pellet as the thylakoid fraction (membrane Fraction). Total protein extraction was conducted as described previously. Proteins were separated by vertical electrophoresis on a 12% (w/v) SDS-polyacrylamide gel and then transferred to a PVDF membrane. The PVDF membrane was incubated with specific antibodies directed against GFP (TransGen Biotech), LHCII, and RBCL. Signals were detected by a Pro-Light HRP Chemiluminescent Kit (Tiangen Biotech).

cDNA synthesis and Real-Time PCR analysis

Total RNA was extracted from frozen tissues ground in liquid nitrogen using the RNeasy Plant Mini Kit (Qiagen) according to the manufacturer's instructions. Subsequently, cDNA was synthesized with the PrimeScript™ RT Reagent Kit (Takara). Real-time PCR analysis was performed as previously described. All experiments were conducted with three biological replicates, each measured in triplicate.

Plant material and growth conditions

Arabidopsis thaliana (ecotype Columbia) was used in this study. Plants were cultivated in soil in a greenhouse, while seeds were germinated and grown on MS medium (1 × MS, pH 5.7, 0.5% sucrose, 0.8% agar) under controlled conditions: a 16-h/8-h light/dark cycle, a light intensity of 120 μmol photons m^{-2} s^{-1}, and a temperature of 22 °C. The *mterf10* mutant (*SALK_097699*) was obtained from the Arabidopsis Biological Resource Center and identified by PCR using genomic DNA and T-DNA specific primers in combination with gene-specific primer [51]. A 20-bp fragment derived from the

coding sequence (CDS; positions 127–146) of *mTERF10* was selected as the target site for genome editing. The designed targeting sequence was cloned into the *Bsa*I-digested AtU6-26-sgRNA-SK vector to generate the AtU6-26-mTERF10-target sgRNA construct. Subsequently, this sgRNA vector was digested with *Nhe*I and *Spe*II, and the released gRNA expression cassette was ligated into the *Spe*I-linearized pYAO: Cas9 backbone, yielding the final binary vector, pYAO: Cas9-*mTERF10*-target sgRNA [52]. The construct was introduced into Agrobacterium tumefaciens strain GV3101 and subsequently transformed into wild-type Arabidopsis thaliana via the floral dip method. Transformants were selected based on hygromycin resistance and confirmed by DNA sequencing. In the T3 generation, Cas9-free plants harboring the desired mutations were identified and used for subsequent experiments.

Results

Plant *mTERF* originated from ancestral plastid *mTERF* through gene duplications and divergence

Given the abundance of mTERF proteins in plants and the well-characterized resources available for *Arabidopsis thaliana*, we selected this species as our model system to investigate mTERF diversification through integrated phylogenetic and molecular analyses. Our phylogenetic reconstruction revealed a strong correlation between evolutionary clustering and subcellular localization. Chloroplast-localized mTERF members (including mTERF1, 2, 3, 4, 5, 6, 8, 9, 10, 11, 12, 16, and 21) [33, 35, 37, 39, 40, 53] formed a single chloroplast-specific clade, whereas mitochondrial-localized members (mTERF13, 14, 20, 28, 29, 30, 31, 32, and 33) [33] were predominantly grouped within mitochondrial-related clades. Additionally, mTERF15, 17, 18, and 35—localized to mitochondria, cytoplasm, or nucleus [33, 41, 54]—constituted a distinct minor clade (Fig. 1A). This strong correlation between phylogenetic clade and organellar localization supports the utility of homology-based localization inference, a complementary approach to algorithmic prediction, for annotating uncharacterized homologs within well-supported clades [55, 56].

To experimentally validate the link between phylogenetic clades and subcellular localization, we performed GFP fusion assays for three mTERF proteins of previously unknown localization: mTERF19, mTERF24, and mTERF34. When co-expressed with the mitochondrial marker FRO1-RFP in protoplasts, all three GFP-tagged proteins showed clear co-localization with the RFP signal, confirming their mitochondrial localization (Fig. 1B).

Conserved motif analysis further supported the functional divergence among mTERF clades. Since no information on structural or functional motifs within the conserved regions was available, we labelled them numerically in order of occurrence from N- to the C-terminal. Proteins in the chloroplast-specific clade commonly shared motifs 2, 1, and 5, while those in mitochondrial-related clades contained a broader set of motifs, including 10, 4, 2, 7, 6, 3, 9, 5, 1, and 8 (Figure S1). Intriguingly, the distinct minor clade, despite sharing subcellular localization with mitochondrial mTERFs, exhibited conserved motifs more similar to those of chloroplast-localized mTERFs. Phylogenetic and motif complexity analyses together suggest an evolutionary trajectory in which the chloroplast-associated clade represents the most ancestral form, followed by the emergence of the distinct minor clade, prior to the diversification of the mitochondrial-localized clades.

Identification and distribution of *mTERF* family members in plant and animals

To validate whether *mTERF* originated and expanded from ancestral choloroplast *mTERFs*, we performed a Hidden Markov Model (HMM)-based search for mTERF protein sequences across available genomes of fungi, metazoans, and plants. Our analysis confirmed the absence of *mTERF* genes in fungal and bacterial genomes, while they were consistently detected in both animal and plant lineages, a finding consistent with prior report [57]. Notably, the *mTERF* gene family exhibits a striking disparity in size between animals and plants. In animals, the family is consistently small, ranging from two to four members across diverse lineages, from basal invertebrates to mammals (Table S1). In contrast, plants have undergone substantial expansion of *mTERF* genes. Two major expansion events were identified during plant evolution: One occurred in the Volvocine algae lineage, where gene numbers rose to approximately 16, likely driven by ancient whole-genome duplication events; the other coincided with the emergence of seed plants, representing a more pronounced expansion that raised the family members to about 51, and was correlated with the ζ and ε whole-genome duplication events (Fig. 2).

To resolve the evolutionary relationships among mTERF proteins, we reconstructed a phylogenetic tree using representative sequences from a range of plant and animal species. Surprisingly, all red algal mTERF proteins clustered within a single clade alongside chloroplast-localized *Arabidopsis* proteins. The distinct minor clade (comprising proteins localized to mitochondria, the nucleus, and the cytoplasm) included mTERFs from Bryophyta, Tracheophyta and a few green algal proteins. In contrast, the mitochondrial-associated clade from *Arabidopsis* contained only seed plants. (Figure S2). These results suggest that plant mTERF proteins likely originated as chloroplast-targeted proteins, and that the distinct minor clade mTERFs subsequently emerged in Embryophytes or late-diverging algae.

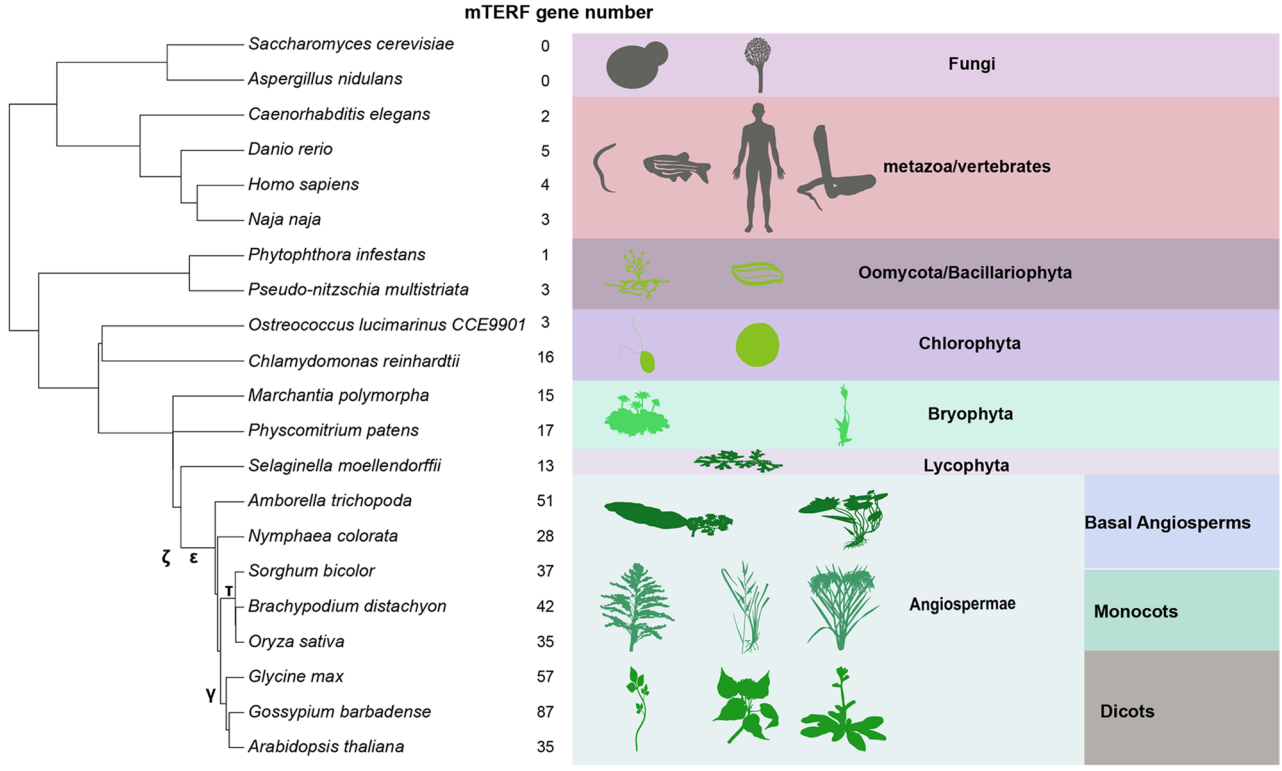

Fig. 2 Phylogenetic distribution of *mTERF* genes in representative eukaryotes. *mTERF* genes were identified from two fungal species, four animal species, and fourteen plant species in this study. The number of *mTERF* genes is displayed between the figure and the phylogenetic tree. The species phylogeny is drawn from timetree. The letters γ, ε, ζ and τ indicate well-established genome duplication events during land plants evolution

Diversification of mTERF proteins in chlorophytes and early land plants

To elucidate the evolutionary trajectory of mTERF proteins during the transition from aquatic algae to land plants, we reconstructed a phylogeny using mTERF sequences from diverse chlorophytes, bryophytes, and representative vascular cryptogams. The analysis resolved three primary clades (A-I, II, III), with Clade A-III subdivided into two well-supported subclades (A-III-1 and A-III-2) (Fig. 3).

Clade A-I was predominantly composed of green algal sequences, identifying it as an ancestral group. Clade A-II contained sequences from both green algae and early land plants (bryophytes and vascular cryptogams), representing a transitional lineage. Clade A-III consisted almost exclusively of early land plant sequences, marking a lineage-specific expansion. Within Clade A-III, subclade A-III-1 showed higher gene copy numbers in vascular cryptogams, whereas subclade A-III-2 was notably expanded in bryophytes (Fig. 3).

In summary, our phylogenetic analysis reveals a key transition in *mTERF* family organization: while vascular plants carried mTERF proteins distributed across multiple clades, the evolutionary lineages from green algae to bryophytes were represented in two clades. Based on their phylogenetic distribution, we propose that the expansion of Clades A-II, A-III-1, and A-III-2 coincided with the evolutionary milestones of land plant terrestrialization, whereas Clade A-I represents the products of earlier expansions within the *mTERF* family prior to the emergence of land plants. These results indicate that the *mTERF* family underwent significant duplication and functional diversification during the transition to terrestrial life. Whole-genome duplications, particularly those identified in Volvox and *Diphasiastrum complanatum*, likely contributed to this expansion.

The emergence of new *mTERF* subfamilies predates the rise of angiosperms

The *mTERF* family exhibits a stepwise increase in gene diversity from algae to bryophytes. To trace its further differentiation in angiosperms, we reconstructed a detailed phylogenetic tree using mTERF sequences from a broad sampling of angiosperm species and a few green algal. The tree resolved two major homologous clades Clade A and Clade B (Fig. 4). Clade A and Clade B in angiosperms possess a similar number of genes (Table S2). These clades further diverged into subclades with distinct phylogenetic patterns: Clade A subclades (A-I/II/III, A-IV) displayed a "species-diverse" structure, comprising a wide range of angiosperms with few genes per species, whereas Clade B subclades (B-I, B-II) exhibited

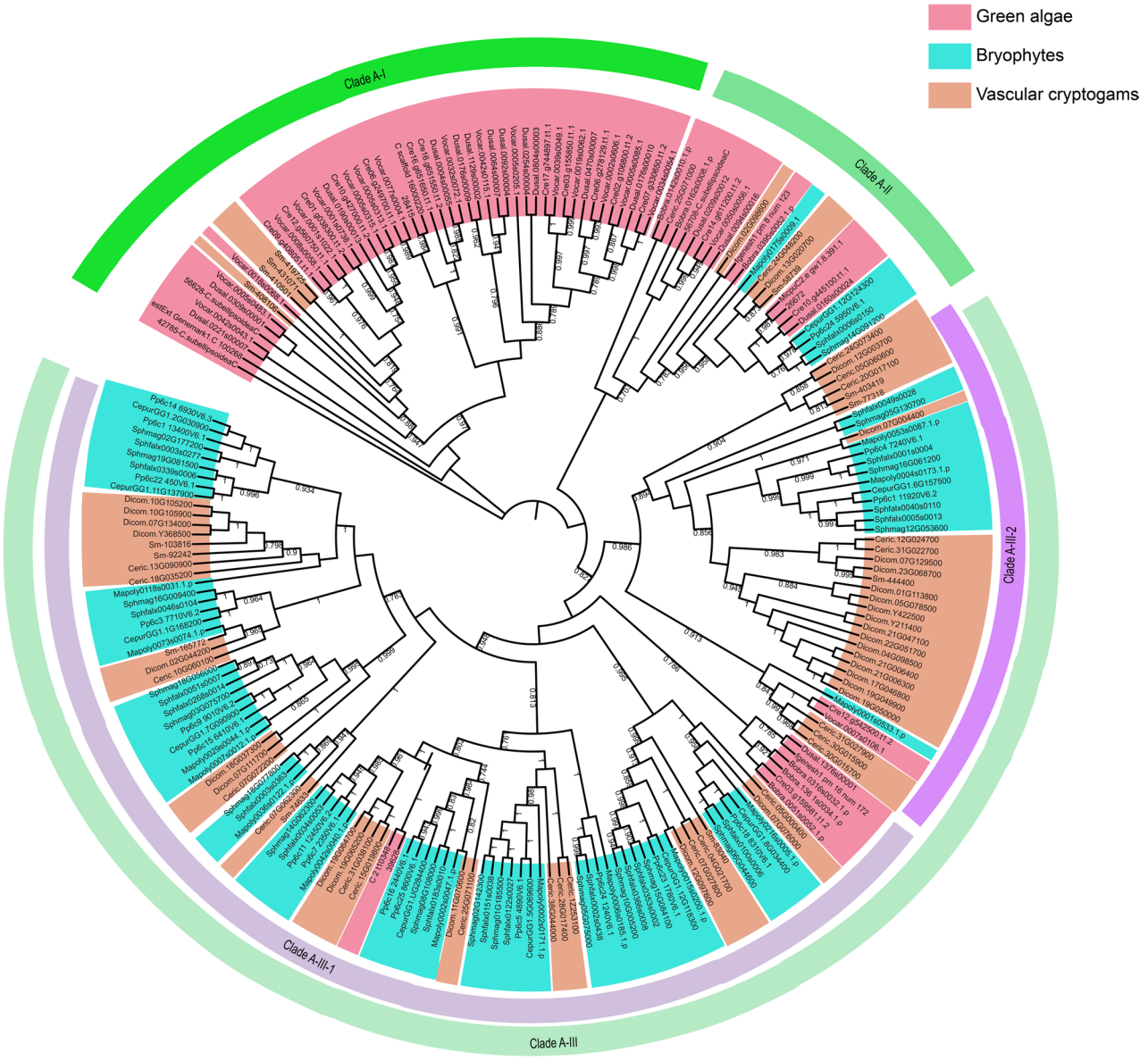

Fig. 3 Phylogenetic relationships of the *mTERF* gene family of the algae and early land plants. A maximum-likelihood tree was constructed using the full-length sequences of 215 mTERF proteins from algae and early land plants in FastTree software. Bootstrap values are indicated at the internal nodes

a "species-specific expansion" pattern, characterized by large gene clusters from individual species (Fig. 4A and B).

Since members of diverse angiosperm lineages are present in both Clade A and Clade B, while all green algal mTERF proteins are exclusively clustered within Clade A (Fig. 4A), it can be inferred that Clade A represents an ancient lineage, and the divergence between these two clades occurred prior to the diversification of angiosperms but subsequent to the emergence of green algae.

To further refine the origin of Clade B, we performed additional phylogenetic analyses using three distinct outgroups: *Amborella trichopoda*, *Selaginella moellendorffii*, and *Physcomitrium*. While mTERFs from the latter two species resided solely within Clade A, those from the basal angiosperm *Amborella* were present in both Clade A and Clade B (Figure S3A-C). This result confirms that Clade B originated after the divergence of vascular plants but prior to the diversification of angiosperms, implicating its potential role in the evolution of seed development.

Gene counts varied considerably among the four angiosperm mTERF clades. Clade B-II contained the most members (167), followed by Clade A-I/II/III (144), Clade B-I (57), and Clade A-IV (52, previously defined as the distinct minor clade localized to mitochondria (Fig. 1) (Table S2). Clades A-IV, and B-I generally contained few genes per species. For example, in monocots such

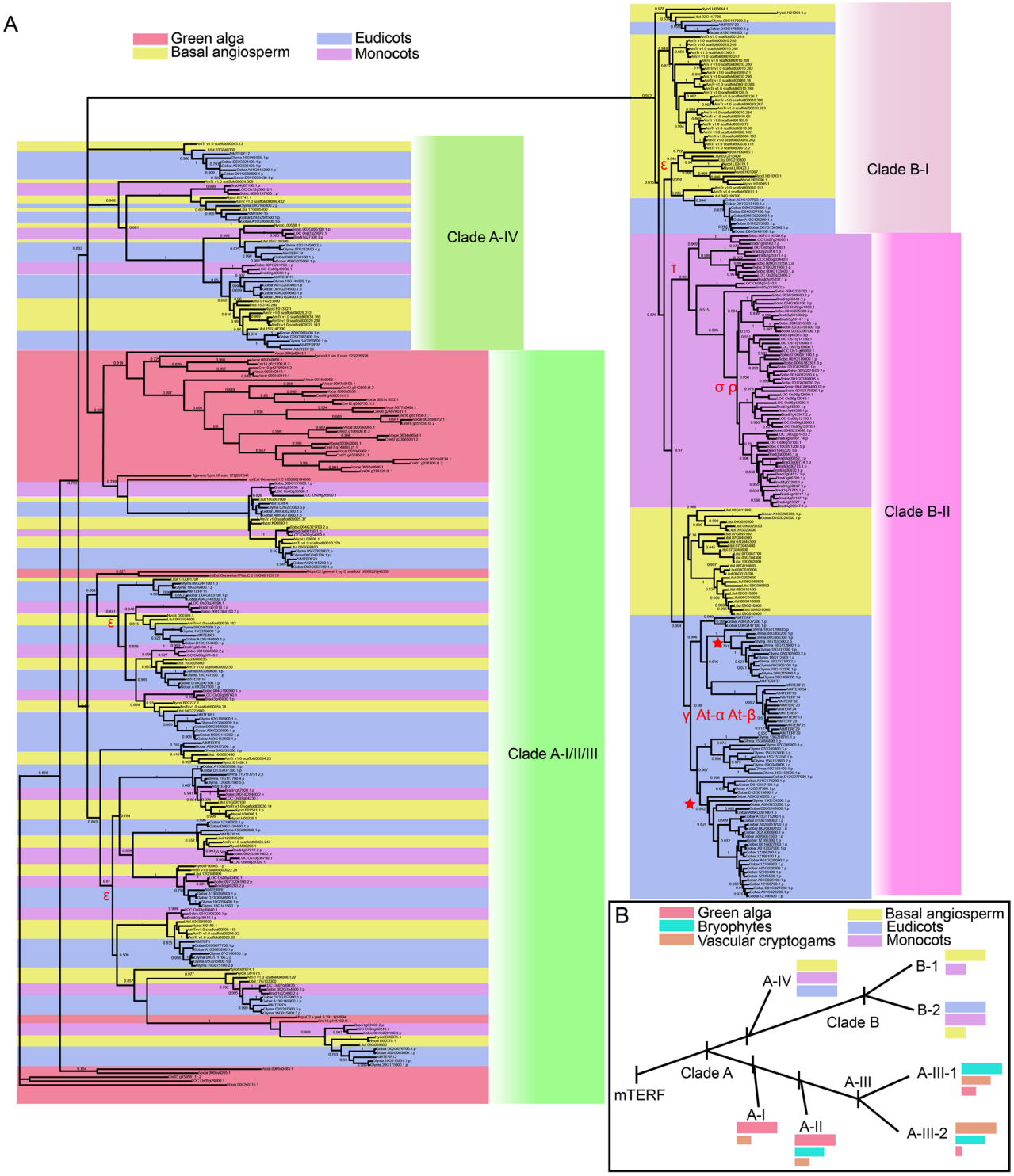

Fig. 4 Phylogenetic relationships of the *mTERF* gene family of angiosperms and chlorophyte

(**A**) Maximum-likelihood phylogenetic tree was inferred from a dataset of 461 protein sequences, including 41 from green algae and 420 from angiosperms. Green algal proteins were included to determine the root and direction of the phylogenetic tree. The two major clades containing the Clade A and Clade B subclass genes are bracketed and labeled, respectively. Letters At-α At-β, γ, ε, ρ, σ, and τ indicate key genome duplication events in land plant evolution, based on tripartite evidence from phylogenomics, molecular clocks, and confirmed duplications in sequenced genomes. Red stars on the tree represents possible

(**B**) Schematic diagram of the phylogenetic relationships of the plant *mTERF* gene family. rectangle size indicates species enrichment level in the clade

as *Oryza sativa*, *Sorghum bicolor*, and *Brachypodium distachyon*, as well as in the early-diverging angiosperm *Nymphaea colorata*, Clades A-IV contain only three gene copies. In the Clade B-I subfamily, monocots are completely absent, while the eudicots including soybean and *Arabidopsis* possess only a single *mTERF* copy with notable exceptions such as *Amborella trichopoda*, cotton (*Gossypium*), and *Nymphaea colorata* (Table S2).

The large number of genes in Clade B-II likely results from repeated gene duplication during evolution. Its expansion appears to have been driven primarily by whole-genome duplication (WGD) and large-scale segmental duplication events (Fig. 4A). Successive WGDs contributed to this amplification, including the angiosperm-wide ε event, the Asteraceae-specific γ event, the Brassicaceae-specific α/β events, the Poaceae-specific σ/ρ events, monocots-specific τ event and independent WGDs in cotton and soybean (Fig. 4A). In contrast to the relatively stable copy number observed in the Clade A subfamily, the newly diverged Clade B subfamily displayed more dynamic and variable gene copy numbers, suggesting a greater degree of functional divergence among its members.

Functional divergence of *mTERFs* between vegetative and reproductive organs in angiosperms

To explore the functional divergence of *mTERF* genes across plant evolution, we analyzed their expression patterns in eight representative species spanning major lineages—*Selaginella moellendorffii*, *Physcomitrium*, *Amborella trichopoda*, *Nymphaea tetragona*, *Oryza sativa*, *Zea mays*, *Arabidopsis thaliana*, and *Glycine max*—using publicly available transcriptome datasets (Fig. 5, Figure S4, Figure S5).

In early land plants, distinct *mTERF* subfamilies exhibited specialized expression profiles. In the lycophyte *Selaginella*, most Clade A-I *mTERF* genes were specifically expressed in roots and rhizophores, whereas this clade was entirely absent in the moss *Physcomitrium*. Clade A-II genes were broadly expressed across multiple tissues in both *P. patens* and *S. moellendorffii*. In contrast, Clade A-III genes showed strong expression specifically in roots and reproductive organs (e.g., spores). Within Clade III, subclade A-III-2 contained more genes than III-1 and displayed more complex expression patterns. In *P. patens*, A-III-2 genes were specifically expressed in roots, chloronema, spores and gametophore. Notably, genes such as *Sm_83040* in *Selaginella* and *PP6C5_4890* in *P. patens* showed broad expression across multiple tissues, underscoring functional diversification within this subclade (Figure S4A).

Following the divergence of early angiosperms, the *mTERF* family split into Clades A and B, with Clade B undergoing pronounced gene expansion. In the basal angiosperms *Amborella* and *Nymphaea*, most Clade A genes were widely expressed across tissues, though only three genes showed such a pattern in *Nymphaea*, with the remainder exhibiting minimal expression. In contrast, Clade B expression was largely restricted to leaves, sepals, carpels, and ovules (Figure S4B).

After the monocot–eudicot split, the *mTERF* gene repertoire was reconfigured, with Clades A and B maintaining similar gene numbers in these lineages. In monocots (rice and maize), some members of Clade A expression were generally higher in vegetative tissues (indicated by Sky-blue stars) than in reproductive organs. Conversely, in rice, a subset of Clade B genes was strongly expressed in reproductive structures such as seeds, embryos, stamens, and pistils (indicated by lavender-blue stars); however, Clade B genes in maize exhibited a broad expression pattern (Fig. 5A, Figure S5A). In eudicots (*Arabidopsis* and soybean), Clade A genes were broadly and highly expressed across most tissues (except pollen). Notably, several highly expressed Clade A genes in *Arabidopsis* have been reported to localize to chloroplasts. Clade B genes, by contrast, generally showed lower expression levels and were preferentially expressed in seeds, embryos, and floral tissues (Fig. 5B). It is noteworthy that the expression levels of *AtmTERF17*, *15*, *18*, *19*, *35*, and *26* from Clade A were higher in reproductive tissues than in vegetative tissues (Fig. 5B). This expression pattern differs from that of most genes in Clade A but resembles the expression profile characteristic of Clade B genes. This is similar to the subcellular localization results mentioned above (Figure S1).

In summary, *mTERF* gene expression diverged markedly between monocots and eudicots: in monocots, some Clade A members predominated in vegetative tissues and Clade B members are broadly expressed or reproductive-enriched, whereas in eudicots, Clade A was broadly highly expressed and a subset of Clade B members remained reproductive-biased. These patterns support functional specialization of *mTERF* clades following the monocot–eudicot divergence. Collinearity analysis further revealed strong conservation of *mTERF* genes within monocots or eudicots, but considerably weaker synteny between these two groups, reinforcing their divergent evolutionary trajectories (Figure S6).

mTERF10 is a negative regulator of thermotolerance in *Arabidopsis*

Transcriptomic analysis revealed distinct expression patterns between the two mTERF clades in *Arabidopsis*: Clade A genes were broadly and highly expressed across all tissues examined, whereas Clade B genes were predominantly expressed in seeds, embryos, and floral tissues (Fig. 5B), suggesting a role for mTERF diversification in plant development. Given previous reports implicating

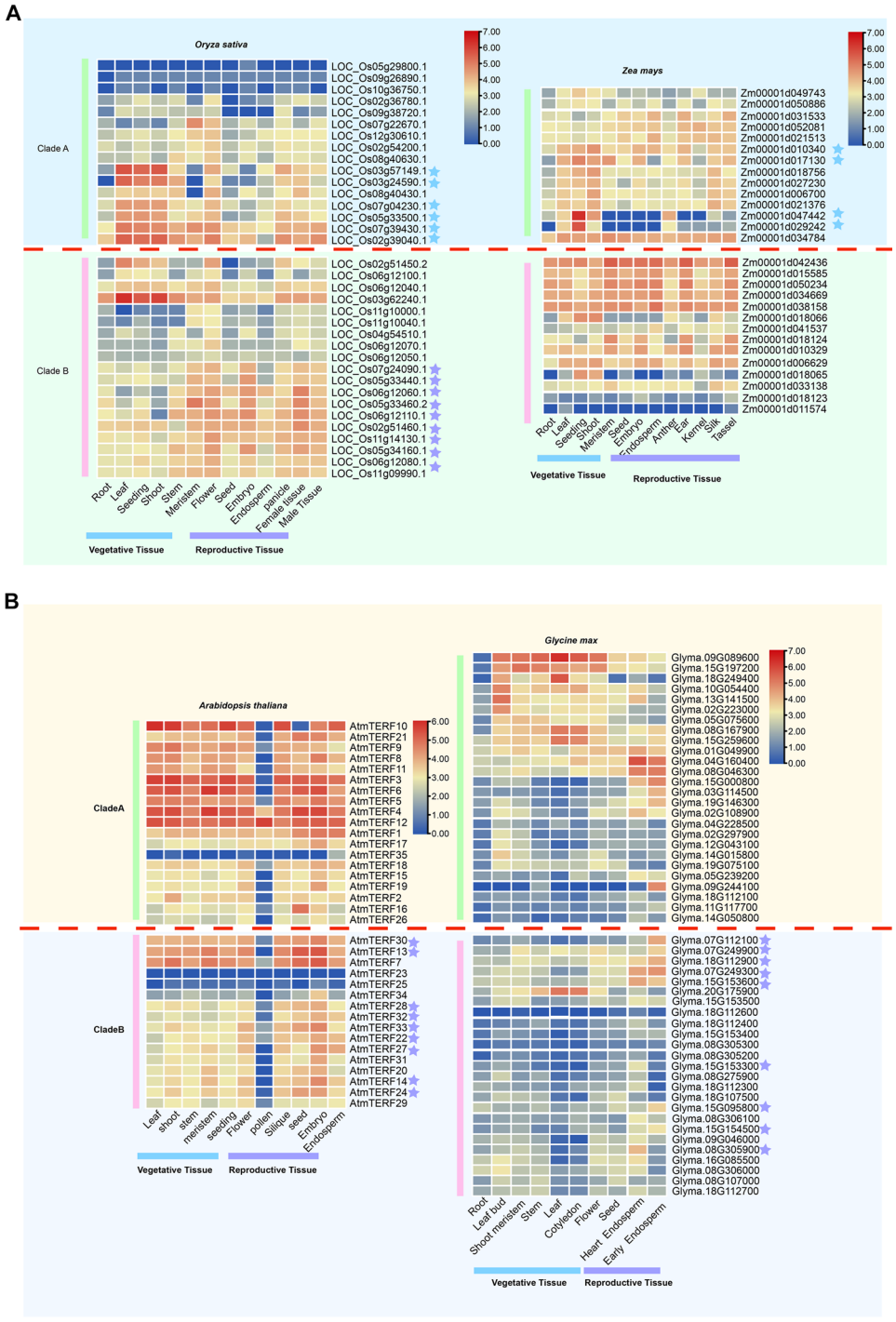

Fig. 5 Expression Heatmap of *mTERF* Genes in Monocot (*Zea mays*, and *Oryza sativa*) (**A**), and Dicot (*Glycine max*, and *Arabidopsis*) (**B**) Across Various Tissues. Based on the phylogenetic classification of *mTERFs* in angiosperms, the expression patterns of Clade A and Clade B are displayed separately. Vegetative and reproductive tissues are indicated with Sky-blue and lavender-blue bars, respectively. The expression matrix (FPKM values) was log2(FPKM + 1)-transformed using TBtools, and the expression heatmaps were subsequently plotted. Sky-blue stars represent genes with high expression in vegetative tissues; lavender-blue stars represent genes with high expression in reproductive tissues

mTERFs in abiotic stress responses, we further investigated whether this functional divergence extends to stress adaptation. Under heat stress (37 °C), most Clade B genes exhibited 2- to 9-fold upregulation, while a subset of Clade A genes (*mTERF2*, *3*, *4*, *15*, and *21*) was also induced, and to a lesser extent (Figure S7A, B). In addition, cold stress (4 °C) elicited similar expression changes in both clades (Figure S7 A, B), indicating the involvement of both subfamilies in the stress response.

However, in our assay of *mTERFs* expression in response to temperature stress, a unique *mTERF*, *mTERF10* came to our attention because its expression was downregulated sharply, distinct to other *mTERFs* (Figure S7A, B). The mTERF10 is found to be localized in chloroplasts in a previous study. Indeed, our mTERF10-GFP fusion protein assay in transgenic plants, together with the immunoblot assay confirm its exclusive localization within chloroplast (Figure S7C, 7D). To investigate the biological function of *mTERF10*, we utilized two independent mutant lines: a T-DNA insertion line (*SALK_097699*, designated *mterf10-1*) obtained from SALK and a CRISPR/Cas9-mediated premature termination mutant (*mterf10-2*) generated in this study (Fig. 6A, B). Under standard growth conditions, both mutants exhibited no visible growth defects or significant alterations in photosynthetic performance, as assessed by light-response curves of electron transport rate (ETR), and non-photochemical quenching (Figure S8). However, under high-temperature stress, the *mterf10* mutant exhibited markedly reduced non-photochemical quenching (NPQ) whereas its photochemical efficiency was enhanced compared to the wild type (Fig. 6C), indicating that mTERF10 negatively regulates temperature response by modulating chloroplast activity.

Discussion

Evolutionary trajectory and functional diversification of mTERF proteins in plants

The mTERF protein family displays a phylogenetically restricted distribution, present in metazoans and plants but absent in fungi and prokaryotes [57]. In contrast to the limited set maintained in metazoans, plants have undergone substantial lineage-specific expansion [58, 59]. Recent research has further revealed that this expansion is closely linked to key plant evolutionary events, such as terrestrial adaptation [60]. Notably, in cereals like wheat and rye, *mTERF* genes have co-expanded and formed clusters with fertility-restorer gene families, directly contributing to the establishment of cytoplasmic male sterility restoration systems [61–63]. Beyond their involvement in fertility, mTERF members play broad roles in regulating organellar gene expression and in adaptive responses to abiotic stresses such as salt, drought, and heat [58, 60]. Our analyses identified two major waves of *mTERF* gene duplication: one in the Volvocine algae, increasing gene number to about 16, and a second coinciding with the rise of seed plants. These findings, partially diverging from earlier reports, likely reflect improved genome assemblies and more comprehensive annotations.

Critically, our phylogenetic reconstructions indicate that plant mTERFs originated from a chloroplast-targeted ancestor, likely present in the last common ancestor of red and green algae (Figure S2). This ancestral clade shares high sequence homology and conserved motifs with chloroplast-localized mTERFs in *Arabidopsis* (Figure S9). Subsequent duplications facilitated the emergence of mitochondrial-targeted paralogs, illustrating a recurrent evolutionary pattern: genes of single organellar origin diversify through duplication to serve both chloroplasts and mitochondria, enabling functional specialization.

An alternative evolutionary scenario is also plausible: mTERF proteins may have originally been targeted to mitochondria. Following endosymbiosis, a subset of these proteins could have been recruited to chloroplasts. Subsequently, the mitochondrial-associated lineage might have been lost or highly diverged in red algae due to genomic reduction, leaving only the plastid-targeted forms detectable today. In green plants, however, both mitochondrial- and plastid-targeted mTERFs were retained and further diversified. Eventually, part of the mitochondrial-targeted clade underwent lineage-specific expansion in angiosperms. Currently, limited by the incomplete genomic data from early-diverging lineages and the scarcity of experimentally validated subcellular localization information, definitively tracing the primordial organellar association of the *mTERF* family remains challenging. This hypothesis offers a fresh perspective for understanding the evolution of organellar regulatory proteins and highlights the need for future studies that integrate broader phylogenomic analyses with cross-lineage functional assays to fully elucidate the evolutionary trajectory of mTERFs in the co-evolution of eukaryotic organelles.

Functional diversification rooted in evolutionary history

The functional divergence of mTERF proteins is deeply rooted in their evolutionary history. In *Arabidopsis*, chloroplast- and mitochondrial-targeted mTERFs form distinct clades, each characterized by specific conserved motifs divergence (Fig. 1, Figure S1). This phylogenetic–functional correlation suggests that early duplication events were followed by neofunctionalization, whereby paralogs acquired distinct subcellular targeting and regulatory roles. Expression analyses further reflect this divergence (Figure S4, Figure S5, Fig. 5). In angiosperms, Clade A *mTERFs* are broadly expressed, suggesting roles

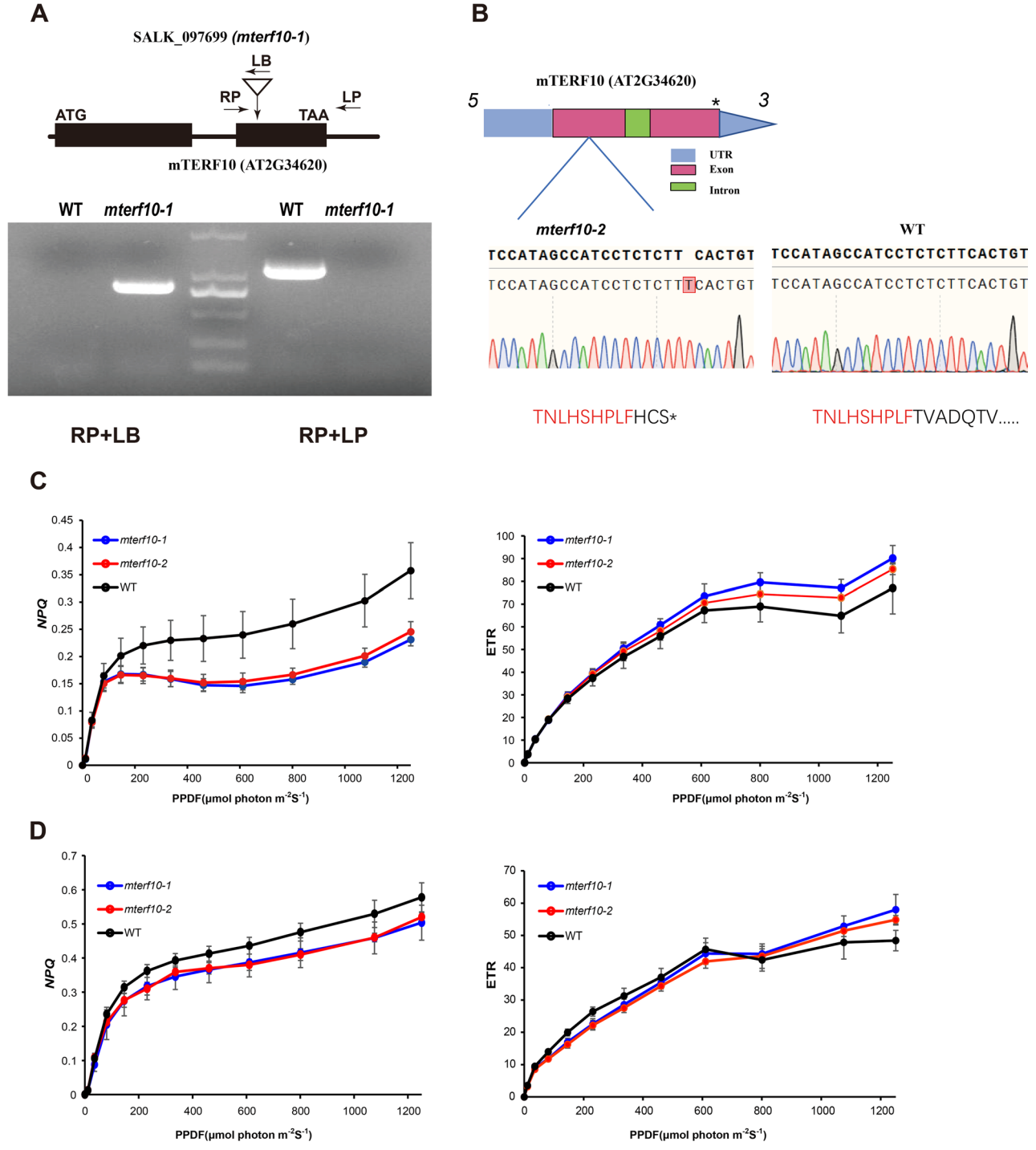

Fig. 6 Characterization of *mterf10* mutants

(**A**) Schematic of the T-DNA insertion site in the *mTERF10* gene. The T-DNA insertion site is indicated by a triangle. Both Left genomic primer (LP) and right genomic primer (RP) are shown. LB represents the left border primer of the T-DNA insertion

(**B**) Verification of the *mterf10-2* homozygous mutant with base insertion via Sanger sequencing of PCR products. The *mterf10-2* homozygous mutant was obtained by CRISPR/Cas9 editing. The left panel shows the sequencing chromatogram of the homozygous mutant with base insertion (resulting in premature protein termination), and the right panel shows the wild-type *mTERF10* sequencing chromatogram as a control

(**C**-**D**) Light-response curves of PSII quantum yield, electron transport rate (ETR), and nonphotochemical quenching (NPQ) in wild-type (WT), *mterf10-1*, and *mterf10-2* mutants following high-temperature treatment at 37 °C (**C**) and cold stress (4 °C) (**D**). Measurements were performed at the following light intensities: 0, 21, 56, 111, 281, 461, 701, 1076, and 1251 μmol m^{-2} s^{-1}. PPFD, photosynthetic photon flux density. Data are presented as mean ± SD. Each data point represents at least 9 independent plants

in basal cellular processes, while Clade B members are enriched in reproductive tissues—a pattern already established in early land plants like *Amborella trichopoda* and *Nymphaea tetragona*. This implies that *mTERF*-mediated regulation of reproduction arose during terrestrial colonization. Notably, high root expression in early lineages that diminished in later angiosperms suggests a historical role in root evolution, inviting future studies on *mTERF* function in root development of non-vascular and early vascular plants.

Several *mTERFs* also contribute to stress adaptation. In *Arabidopsis*, mutants of *mterf18/shot1* and *mterf1* (*soldat10*) respectively confer enhanced tolerance to heat/oxidative stress and significantly higher seed germination under salt stress compared to the wild type [53, 54]. mTERF10, a chloroplast stromal protein negatively regulating thermotolerance, shares highest similarity with human mTERF3, a transcriptional repressor [64]. We propose that mTERF10 may similarly repress chloroplast gene transcription, and its downregulation under stress may enhance photosynthetic gene expression. It is previously characterized as a positive regulator of salt stress response [65]. This functional diversity underscores how conserved regulatory mechanisms can be repurposed in different organelles and organisms in responding to distinct stress.

In summary, the *mTERF* family exemplifies how repeated gene duplication and neofunctionalization enable nuclear-encoded factors to regulate both chloroplast and mitochondrial functions, supporting plant adaptation to developmental and environmental challenges.

Conclusion

This study elucidates the evolutionary trajectory of mTERF proteins in plants and identifies mTERF10 as a negative regulator of temperature stress. Compared to animals, the plant mTERF family has undergone significant lineage-specific expansion. This study identified two significant episodes in plant mTERFs evolution: origins most likely as chloroplast-targeted members in the Archaeplastidal ancestor (shared by red algae and chlorophytes) and subsequent duplication, divergence and potential neofunctionalization that gave rise to a subfamily of mitochondria-targeted members unique to seed-plants. Different mTERF lineages regulate distinct biological processes, including reproductive development, stress responses, and vegetative growth. Genetic analysis demonstrates that mTERF10 acts as a negative regulator of thermotolerance, revealing how the same protein family can evolve neofunctionalization to enable plants to cope with varying environmental stresses. Our findings provide novel insights into the co-evolution of nuclear and organellar genomes and the regulatory plasticity underlying plant adaptation.

Abbreviations

mTERF	Mitochondrial transcription termination factor
PPR	Pentatricopeptide repeat proteins
ETR	Light-response curves of electron transport rate
WGD	whole-genome duplication
ML	Maximum likelihood
HMM	Hidden Markov Model

Supplementary Information

The online version contains supplementary material available at https://doi.org/10.1186/s12870-026-08328-w.

Supplementary Material 1.

Supplementary Material 2.

Acknowledgements

We gratefully acknowledge Dr. Xintong Xu from Peking University for his valuable assistance with the bioinformatics analysis.

Authors' contributions

WC designed the research. LY, LJY and WC analyzed and interpreted data and drafted the manuscript. LY, XSW and HL assisted in the visualization and finalization of figures. WC critically revised the manuscript.Declarations, Ethics approval and consent to participate, Not applicable.Consent for publication, Not applicable.Competing interests, The authors declare that there are no competing interests.Data Availability, The datasets generated or analyzed during this study are available in the published article or supplementary materials.

Funding

This work was supported by National Key Research and Development Program (grant nos. 2021YFA1300400 and 2022YFF1001700), China Postdoctoral Science Foundation (2025M782662) and the Natural Science Foundation of Jiangsu Province (BK20250004).

Data availability

Data AvailabilityThe datasets generated or analyzed during this study are available in this published article or supplementary materials.

Declarations

Ethics approval and consent to participate

Not applicable.

Consent for publication

Not applicable.

Competing interests

The authors declare no competing interests.

Received: 21 December 2025 / Accepted: 3 February 2026
Published online: 07 February 2026

References

1. Sagan L. On the origin of mitosing cells. J Theor Biol. 1967;14(3):225. ,IN221-274,IN226.
2. Zimorski V, Ku C, Martin WF, Gould SB. Endosymbiotic theory for organelle origins. Curr Opin Microbiol. 2014;22:38–48.
3. Archibald JM. Endosymbiosis and eukaryotic cell evolution. Curr Biol. 2015;25(19):R911–921.
4. Petitjean C, Williams TA. Evolution: new Gene-Rich mitochondria found across the eukaryotic tree. Curr Biol. 2017;27(23):R1270–1.

5. Butenko A, Lukeš J, Speijer D, Wideman JG. Mitochondrial genomes revisited: why do different lineages retain different genes? BMC Biol. 2024;22(1):15.
6. Bock R. Witnessing genome evolution: experimental reconstruction of endosymbiotic and horizontal gene transfer. Annu Rev Genet. 2017;51:1–22.
7. Nishimura K, van Wijk KJ. Organization, function and substrates of the essential Clp protease system in plastids. Biochim Biophys Acta. 2015;1847(9):915–30.
8. Yu AY, Houry WA. ClpP: a distinctive family of cylindrical energy-dependent Serine proteases. FEBS Lett. 2007;581(19):3749–57.
9. Richardson LGL, Schnell DJ. Origins, function, and regulation of the TOC-TIC general protein import machinery of plastids. J Exp Bot. 2020;71(4):1226–38.
10. Sloan DB, Warren JM, Williams AM, Wu Z, Abdel-Ghany SE, Chicco AJ, Havird JC. Cytonuclear integration and co-evolution. Nat Rev Genet. 2018;19(10):635–48.
11. Miyagishima SY. Mechanism of plastid division: from a bacterium to an organelle. Plant Physiol. 2011;155(4):1533–44.
12. Vosseberg J, van Hooff JJE, Köstlbacher S, Panagiotou K, Tamarit D, Ettema TJG. The emerging view on the origin and early evolution of eukaryotic cells. Nature. 2024;633(8029):295–305.
13. Singer A, Poschmann G, Mühlich C, Valadez-Cano C, Hänsch S, Hüren V, Rensing SA, Stühler K, Nowack ECM. Massive protein import into the Early-Evolutionary-Stage photosynthetic organelle of the amoeba paulinella chromatophora. Curr Biol. 2017;27(18):2763–e27732765.
14. Roger AJ, Muñoz-Gómez SA, Kamikawa R. The origin and diversification of mitochondria. Curr Biol. 2017;27(21):R1177–92.
15. Small I, Melonek J, Bohne AV, Nickelsen J, Schmitz-Linneweber C. Plant organellar RNA maturation. Plant Cell. 2023;35(6):1727–51.
16. Hammani K, Giegé P. RNA metabolism in plant mitochondria. Trends Plant Sci. 2014;19(6):380–9.
17. Barkan A, Small I. Pentatricopeptide repeat proteins in plants. Annu Rev Plant Biol. 2014;65:415–42.
18. Gutmann B, Royan S, Schallenberg-Rüdinger M, Lenz H, Castleden IR, McDowell R, Vacher MA, Tonti-Filippini J, Bond CS, Knoop V, et al. The expansion and diversification of pentatricopeptide repeat RNA-Editing factors in plants. Mol Plant. 2020;13(2):215–30.
19. Quesada V. The roles of mitochondrial transcription termination factors (MTERFs) in plants. Physiol Plant. 2016;157(3):389–99.
20. Jalal A, Schwarz C, Schmitz-Linneweber C, Vallon O, Nickelsen J, Bohne AV. A small multifunctional pentatricopeptide repeat protein in the Chloroplast of chlamydomonas reinhardtii. Mol Plant. 2015;8(3):412–26.
21. Hammani K, Takenaka M, Miranda R, Barkan A. A PPR protein in the PLS subfamily stabilizes the 5′-end of processed rpl16 mRNAs in maize chloroplasts. Nucleic Acids Res. 2016;44(9):4278–88.
22. Zhelyazkova P, Hammani K, Rojas M, Voelker R, Vargas-Suárez M, Börner T, Barkan A. Protein-mediated protection as the predominant mechanism for defining processed mRNA termini in land plant chloroplasts. Nucleic Acids Res. 2012;40(7):3092–105.
23. Prikryl J, Rojas M, Schuster G, Barkan A. Mechanism of RNA stabilization and translational activation by a pentatricopeptide repeat protein. Proc Natl Acad Sci U S A. 2011;108(1):415–20.
24. Schmitz-Linneweber C, Williams-Carrier R, Barkan A. RNA Immunoprecipitation and microarray analysis show a Chloroplast pentatricopeptide repeat protein to be associated with the 5′ region of mRNAs whose translation it activates. Plant Cell. 2005;17(10):2791–804.
25. Meierhoff K, Felder S, Nakamura T, Bechtold N, Schuster G. HCF152, an Arabidopsis RNA binding pentatricopeptide repeat protein involved in the processing of Chloroplast psbB-psbT-psbH-petB-petD RNAs. Plant Cell. 2003;15(6):1480–95.
26. Fujii S, Small I. The evolution of RNA editing and pentatricopeptide repeat genes. New Phytol. 2011;191(1):37–47.
27. Rüdinger M, Polsakiewicz M, Knoop V. Organellar RNA editing and plant-specific extensions of pentatricopeptide repeat proteins in Jungermanniid but not in marchantiid liverworts. Mol Biol Evol. 2008;25(7):1405–14.
28. Saha D, Prasad AM, Srinivasan R. Pentatricopeptide repeat proteins and their emerging roles in plants. Plant Physiol Biochem. 2007;45(8):521–34.
29. Wang Y, Tan BC. Pentatricopeptide repeat proteins in plants: cellular functions, action mechanisms, and potential applications. Plant Commun. 2025;6(2):101203.
30. Hyvärinen AK, Pohjoismäki JL, Reyes A, Wanrooij S, Yasukawa T, Karhunen PJ, Spelbrink JN, Holt IJ, Jacobs HT. The mitochondrial transcription termination factor mTERF modulates replication pausing in human mitochondrial DNA. Nucleic Acids Res. 2007;35(19):6458–74.
31. Martin M, Cho J, Cesare AJ, Griffith JD, Attardi G. Termination factor-mediated DNA loop between termination and initiation sites drives mitochondrial rRNA synthesis. Cell. 2005;123(7):1227–40.
32. Yakubovskaya E, Mejia E, Byrnes J, Hambardjieva E, Garcia-Diaz M. Helix unwinding and base flipping enable human MTERF1 to terminate mitochondrial transcription. Cell. 2010;141(6):982–93.
33. Babiychuk E, Vandepoele K, Wissing J, Garcia-Diaz M, De Rycke R, Akbari H, Joubès J, Beeckman T, Jänsch L, Frentzen M, et al. Plastid gene expression and plant development require a plastidic protein of the mitochondrial transcription termination factor family. Proc Natl Acad Sci U S A. 2011;108(16):6674–9.
34. Quesada V, Sarmiento-Mañús R, González-Bayón R, Hricová A, Pérez-Marcos R, Graciá-Martínez E, Medina-Ruiz L, Leyva-Díaz E, Ponce MR, Micol JL. Arabidopsis RUGOSA2 encodes an mTERF family member required for mitochondrion, Chloroplast and leaf development. Plant J. 2011;68(4):738–53.
35. Ding S, Zhang Y, Hu Z, Huang X, Zhang B, Lu Q, Wen X, Wang Y, Lu C. mTERF5 acts as a transcriptional pausing factor to positively regulate transcription of Chloroplast PsbEFLJ. Mol Plant. 2019;12(9):1259–77.
36. Méteignier LV, Ghandour R, Meierhoff K, Zimmerman A, Chicher J, Baumberger N, Alioua A, Meurer J, Zoschke R, Hammani K. The Arabidopsis mTERF-repeat MDA1 protein plays a dual function in transcription and stabilization of specific Chloroplast transcripts within the PsbE and NdhH operons. New Phytol. 2020;227(5):1376–91.
37. Romani I, Manavski N, Morosetti A, Tadini L, Maier S, Kühn K, Ruwe H, Schmitz-Linneweber C, Wanner G, Leister D, et al. A member of the Arabidopsis mitochondrial transcription termination factor family is required for maturation of Chloroplast transfer RNAIle(GAU). Plant Physiol. 2015;169(1):627–46.
38. Zhang Y, Cui YL, Zhang XL, Yu QB, Wang X, Yuan XB, Qin XM, He XF, Huang C, Yang ZN. A nuclear-encoded protein, mTERF6, mediates transcription termination of RpoA Polycistron for plastid-encoded RNA polymerase-dependent Chloroplast gene expression and Chloroplast development. Sci Rep. 2018;8(1):11929.
39. Xiong HB, Wang J, Huang C, Rochaix JD, Lin FM, Zhang JX, Ye LS, Shi XH, Yu QB, Yang ZN. mTERF8, a member of the mitochondrial transcription termination factor Family, is involved in the transcription termination of Chloroplast gene PsbJ. Plant Physiol. 2020;182(1):408–23.
40. Méteignier LV, Ghandour R, Zimmerman A, Kuhn L, Meurer J, Zoschke R, Hammani K. Arabidopsis mTERF9 protein promotes Chloroplast ribosomal assembly and translation by Establishing ribonucleoprotein interactions in vivo. Nucleic Acids Res. 2021;49(2):1114–32.
41. Hsu YW, Wang HJ, Hsieh MH, Hsieh HL, Jauh GY. Arabidopsis mTERF15 is required for mitochondrial nad2 intron 3 splicing and functional complex I activity. PLoS ONE. 2014;9(11):e112360.
42. Hammani K, Barkan A. An mTERF domain protein functions in group II intron splicing in maize chloroplasts. Nucleic Acids Res. 2014;42(8):5033–42.
43. Eddy SR, Pearson WR. Accelerated profile HMM searches. PLoS Comput Biol. 2011;7(10):e1002195.
44. Zhang H, Zhang F, Yu Y, Feng L, Jia J, Liu B, Li B, Guo H, Zhai J. A comprehensive online database for exploring ~20,000 public Arabidopsis RNA-Seq libraries. Mol Plant. 2020;13(9):1231–3.
45. Yang Z, Luo C, Pei X, Wang S, Huang Y, Li J, Liu B, Kong F, Yang QY, Fang C. SoyMD: a platform combining multi-omics data with various tools for soybean research and breeding. Nucleic Acids Res. 2024;52(D1):D1639–50.
46. Guo Z, Luo S, Wang Q, Yang Y, Bai Y, Wei J, Wang D, Duan Y, Yang X, Yang Y. ANAgdb: a multi-omics and taxonomy database for ANA-grade. BMC Plant Biol. 2024;24(1):882.
47. Ortiz-Ramírez C, Hernandez-Coronado M, Thamm A, Catarino B, Wang M, Dolan L, Feijó JA, Becker JD. A transcriptome atlas of physcomitrella patens provides insights into the evolution and development of land plants. Mol Plant. 2016;9(2):205–20.
48. Mello A, Efroni I, Rahni R, Birnbaum KD. The selaginella rhizophore has a unique transcriptional identity compared with root and shoot meristems. New Phytol. 2019;222(2):882–94.
49. Kovtun Y, Chiu WL, Tena G, Sheen J. Functional analysis of oxidative stress-activated mitogen-activated protein kinase cascade in plants. Proc Natl Acad Sci U S A. 2000;97(6):2940–5.
50. Clough SJ, Bent AF. Floral dip: a simplified method for Agrobacterium-mediated transformation of Arabidopsis Thaliana. Plant J. 1998;16(6):735–43.
51. Alonso, José M, Stepanova, Anna N, Leisse, Thomas J. Kim: Genome-Wide Insertional Mutagenesis of Arabidopsis thaliana. Science. 2003;301(5633):653–7.

52. Yan L, Wei S, Wu Y, Hu R, Li H, Yang W, Xie Q. High-Efficiency genome editing in Arabidopsis using YAO Promoter-Driven CRISPR/Cas9 system. Mol Plant. 2015;8(12):1820–3.
53. Meskauskiene R, Würsch M, Laloi C, Vidi PA, Coll NS, Kessler F, Baruah A, Kim C, Apel K. A mutation in the Arabidopsis mTERF-related plastid protein SOLDAT10 activates retrograde signaling and suppresses 1O2-induced cell death. Plant J. 2009;60(3):399–410.
54. Kim M, Schulz V, Brings L, Schoeller T, Kühn K, Vierling E. mTERF18 and ATAD3 are required for mitochondrial nucleoid structure and their disruption confers heat tolerance in Arabidopsis Thaliana. New Phytol. 2021;232(5):2026–42.
55. Adelfio A, Volpato V, Pollastri G. SCLpredT: Ab initio and homology-based prediction of subcellular localization by N-to-1 neural networks. Springerplus. 2013;2:502.
56. Gould SB, Magiera J, García García C, Raval PK. Reliability of plastid and mitochondrial localisation prediction declines rapidly with the evolutionary distance to the training set increasing. PLoS Comput Biol. 2024;20(11):e1012575.
57. Roberti M, Polosa PL, Bruni F, Manzari C, Deceglie S, Gadaleta MN, Cantatore P. The MTERF family proteins: mitochondrial transcription regulators and beyond. Biochim Biophys Acta. 2009;1787(5):303–11.
58. Kleine T, Leister D. Emerging functions of mammalian and plant mTERFs. Biochim Et Biophys Acta (BBA) - Bioenergetics. 2015;1847(9):786–97.
59. Kleine T. Arabidopsis Thaliana mTERF proteins: evolution and functional classification. Front Plant Sci. 2012;3:233.
60. P KR, MacLeod AI, Gould SB. A molecular atlas of plastid and mitochondrial proteins reveals organellar remodeling during plant evolutionary transitions from algae to angiosperms. PLoS Biol. 2024;22(5):e3002608.
61. Walkowiak S, Gao L, Monat C, Haberer G, Kassa MT, Brinton J, Ramirez-Gonzalez RH, Kolodziej MC, Delorean E, Thambugala D, et al. Multiple wheat genomes reveal global variation in modern breeding. Nature. 2020;588(7837):277–83.
62. Melonek J, Small I. Triticeae genome sequences reveal huge expansions of gene families implicated in fertility restoration. Curr Opin Plant Biol. 2022;66:102166.
63. Rabanus-Wallace MT, Hackauf B, Mascher M, Lux T, Wicker T, Gundlach H, Baez M, Houben A, Mayer KFX, Guo L, et al. Chromosome-scale genome assembly provides insights into Rye biology, evolution and agronomic potential. Nat Genet. 2021;53(4):564–73.
64. Park CB, Asin-Cayuela J, Cámara Y, Shi Y, Pellegrini M, Gaspari M, Wibom R, Hultenby K, Erdjument-Bromage H, Tempst P, et al. MTERF3 is a negative regulator of mammalian MtDNA transcription. Cell. 2007;130(2):273–85.
65. Xu D, Leister D, Kleine T: Arabidopsis thaliana mTERF10 and mTERF11, but Not mTERF12, Are Involved in the Response to Salt Stress. Front Plant Sci. 2017;8:1213.

Publisher's note